Heliyon 10 (2024) e30337

Contents lists available at ScienceDirect

Heliyon

journal homepage: www.cell.com/heliyon

Research article

Establishment of a novel efferocytosis potential index predicts prognosis and immunotherapy response in cancers

Peng Chen [a], Zhanzhan Li [b], Na Li [b,*]

[a] Department of Orthopedics, Xiangya Hospital, Central South University, Changsha, 410008, Hunan Province, China
[b] Department of Oncology, Xiangya Hospital, Central South University, Changsha, Hunan Province, 410008, China

ARTICLE INFO

Keywords:
Efferocytosis
Pan-cancer
Prognosis
Immunotherapy
Immune infiltration

ABSTRACT

The biological function and prognostic value of efferocytosis in cancer remains unclear. In this study, we systematically analysed the expression profiles and genetic variations of 50 efferocytosis-related regulator genes in 33 cancer types. Using data from The Cancer Genome Atlas, we established an efferocytosis potential index (EPI) model to represent the efferocytosis level in each cancer type. The relationship between the EPI and prognosis, immune-related molecules, specific pathways, and drug sensitivity was determined. We found that efferocytosis regulator genes were abnormally expressed in cancer tissue, perhaps owing to copy number variations, gene alterations, and DNA methylation. For the most part, the EPI was higher in tumour vs. normal tissues. In most of the 33 cancer types, it positively correlated with cell death- and immune-related pathway enrichment, the tumour microenvironment, immune infiltration, and drug sensitivity. For specific cancers, a high EPI may be a prognostic risk factor and, in patients treated receiving immune checkpoint therapy, a predictor of poor prognosis. Our study reveals the biological functions of efferocytosis-related regulator genes in distinct cancers and highlights the potential of efferocytosis intervention in cancer therapy.

1. Introduction

Regular cell turnover is fundamental for maintaining health. The estimated rate of turnover is approximately 80 ± 20 g of cellular mass per day [1]. Few apoptotic cells (ACs) are normally observed in tissues, implying their efficient clearance by a process termed efferocytosis. Efferocytosis is crucial for homeostasis. When defective, dead cells accumulate, and release of their contents into their surroundings may cause secondary necrosis [2–4] and consequent inflammation-related diseases, such as atherosclerosis, age-associated inflammation, infectious diseases, systemic lupus erythematosus, obesity, and cancer [5].

The mechanisms and processes of efferocytosis are complex. First, phagocytic cells migrate to ACs when sensing graduated signals released by ACs, such as the lipids lysophosphatidylcholine and sphingosine 1-phosphate, the fractalkine CX3CL1, and the nucleotides ATP and UTP [6]. Second, phagocytes recognize "eat-me" signals, which are usually unique markers on the AC's surface. These include phosphatidylserine (PS), which is confined to the inner leaflet of the plasma membrane in normal cells but exposed on the outer membrane in dying cells [7]. By directly or indirectly binding to PS, phagocytes initiate the engulfment and digestion of ACs. Living cells do not express eat-me signals and thus are not engulfed [8,9]. Additional eat-me signals include CD24, CD31, and CD47.

The immune system plays an essential role in the surveillance, recognition, and eradication of normally turned over cells and

* Corresponding author. No.87, Xiangya Road, Kaifu District, Changsha, Hunan Province, 410008, China.
E-mail address: nali0702@csu.edu.cn (N. Li).

https://doi.org/10.1016/j.heliyon.2024.e30337
Received 9 October 2023; Received in revised form 23 April 2024; Accepted 24 April 2024
Available online 25 April 2024

nascent cancer cells. However, many cancer cells use various methods to avoid immune surveillance and immunological killing and thus survive and proliferate [10]. Efferocytosis facilitates cancer development by swiftly clearing dead cells and releasing anti-inflammatory cytokines to create an immunosuppressive tumour microenvironment (TME) [11–13]. Phagocytic macrophages are recruited to the TME and become M2-polarized tumour-associated macrophages. M2-polarized macrophages release anti-inflammatory mediators to help the tumour escape surveillance at multiple cancer stages, including initiation, progression, metastasis, and angiogenesis [14–16]. Therefore, targeting their receptors or blocking their formation may be an attractive intervention for cancer treatment.

Investigation of efferocytosis-related signal pathways has identified several potential targets for intervention. The most notable targets are the TAM receptors (Tyro3, Axl, and MerTK) on macrophages. These receptors recognize PS on ACs using Gas6 and protein S as bridging ligands and thereby promote efferocytosis to create a tumour-tolerant environment [17]. Overexpression of TAM receptors has been implicated in various cancers, such as hepatocellular carcinoma, colorectal cancer, non-small cell lung cancer, melanoma, and gastric cancer [18–24]. When released from tumour macrophages into the TCM, the anti-inflammatory cytokines transforming growth factor β and interleukin (IL)-10 attenuate pro-inflammatory responses and contribute to drug resistance [25]. In view of the complex immune-related events and promising targets in efferocytosis, we believe that a systematic analysis of efferocytosis in various cancers would help us further uncover its underlying mechanisms and optimize cancer treatments. In this study, we evaluated the expression profiles and variation status of 50 efferocytosis-related regulator genes in 33 cancer types. We established an efferocytosis potential index (EPI) model using single sample gene set enrichment analysis (ssGSEA) based on enrichment score to describe the efferocytosis levels of the cancers. Associations between the EPI and 1) biological signalling pathways, especially those involving immune-related molecules and events, 2) clinical outcome endpoints, most notably, the immunotherapy response and overall survival (OS), and 3) drug sensitivity were investigated. In summary, our study reveals a fundamental involvement of efferocytosis in cancer, and as such, may improve cancer therapy, especially immunotherapy.

2. Materials and methods

2.1. Data source and differential gene expression analysis

We downloaded the RNA-seq (HTSeq) data for 33 cancer and normal tissues, along with their corresponding clinical parameters, from the University of California, Santa Cruz (https://xenabrowser.net/datapages/). The limma R package was used to analyse the differential expression of 50 efferocytosis-related regulator genes among the cancer types [26]. Significant differences in expression were defined as $|\log FC| > 1$, $p < 0.05$. The genes and cancer types are listed in Tables S1 and S2.

2.2. Genetic variation, methylation analysis, and protein-protein interaction analysis

Single nucleotide variation (SNV), copy number variation (CNV), and gene methylation were analysed using the Gene Set Cancer Analysis database (http://bioinfo.life.hust.edu.cn/GSCA/#/). Pearson's correlation coefficient was used to examine correlations between CNV or methylation and mRNA expression. Protein-protein interaction was analysed using Cytoscape software using data downloaded from the STRING website (https://cn.string-db.org/).

2.3. Establishment of the EPI model in pan-cancer

We generated an EPI for each cancer type using ssGSEA based on enrichment score. The EPI represents the efferocytosis level, and the enrichment score represents the proportion of each of the 50 efferocytosis-related regulator genes in the sample. R GSEABase packages were used for calculations.

2.4. Survival analysis

The association between the EPI and clinical endpoints was assessed using Cox regression analysis. The endpoints were OS, progression-free interval (PFI), disease-specific survival (DSS), and disease-free interval (DFI). Kaplan–Meier survival analysis was used to determine the survival probabilities of the patients. $P < 0.05$ was considered significant.

2.5. Correlation of the EPI with tumour mutational burden (TMB), microsatellite instability (MSI), and immune infiltration

Immune-associated data were downloaded from the Immune Cell Abundance Identifier database (http://bioinfo.life.hust.edu.cn/ImmuCellAI/#!/). The Estimation of STromal and Immune cells in MAlignant Tumour tissues (ESTIMATE) algorithm was used to approximate the levels of immune components and overall stroma [27]. Pearson's correlation coefficient was used to assess the relevance of the EPI to TMB; MSI; immune parameters (stromal, immune, and ESTIMATE scores); and the expression of immune checkpoint, immunostimulatory, immunosuppressive, and major histocompatibility complex (MHC), chemokine, and chemokine receptor genes. The correlation between the EPI and Tumour Immune Dysfunction and Exclusion (TIDE) score was evaluated in the cancers. Three immunotherapy cohorts [IMvigor210, GSE32894, and NCT02684006 (PMID: 32895571)] were used to validate the effect of the EPI on immunotherapy outcomes.

2.6. Correlation of the EPI and drug sensitivity in pan-cancer

Drug response data were obtained from Genomics of Drug Sensitivity in Cancer (https://www.cancerrxgene.org/) and the Cancer Therapeutics Response Portal (https://portals.broadinstitute.org/ctrp/). Pearson's correlation coefficient was used to assess the association between the EPI and small-molecule drug sensitivity.

3. Results

3.1. Landscape of efferocytosis regulators in pan-cancer

To better understand the relationship between efferocytosis and cancer, we evaluated the mRNA expression of 50 efferocytosis-related regulator genes in 33 cancer types and established an EPI model (Fig. 1). *C1QA* and *RAC1* were highly expressed, whereas *ADGRB1*, *STAB2*, and *TIMD4* had relatively low expression levels (Fig. 2A).

CNV, a major genetic structural variation, has been shown to closely correlate with the expression of most genes, indicating their possible regulation in disease-related pathways [28]. In our study, this correlation was observed for a few regulator genes, including *PTDSS1*, *RAC1*, *DNM1L*, *RUBCN*, and *PANX1* (positive correlation in more than 25 cancer types) (Fig. 2B). Further analysis of heterozygous and homozygous CNVs showed that most of the regulator genes had heterozygous amplifications or deletions (Fig. S1).

Genetic sequence variation was examined in the 33 cancer types. Among the 2947 cancer samples, 1845 (62.61 %) harboured sequence variations; missense mutations were most frequently seen. Fig. 2C and D lists the top 10 mutated genes; notably, one of these

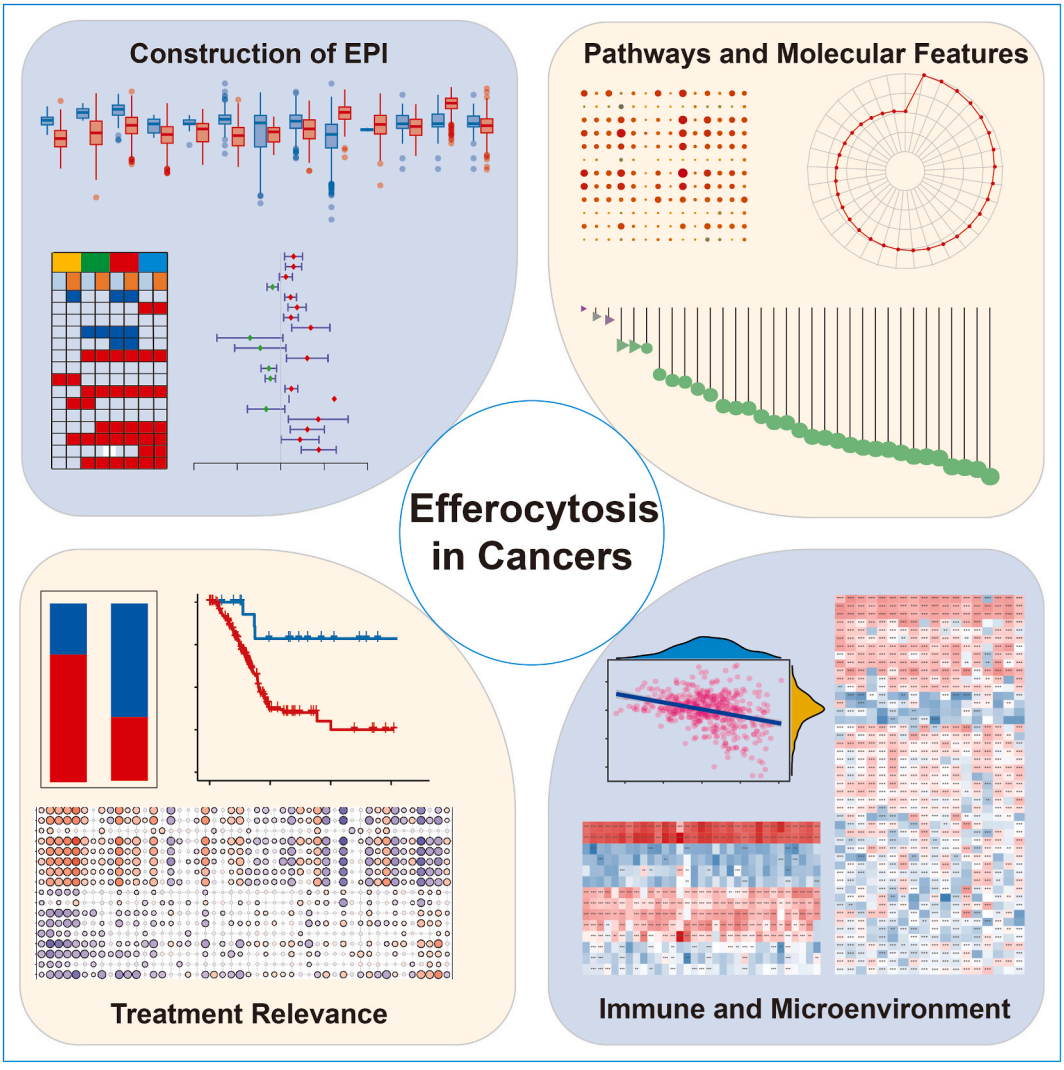

Fig. 1. Flow chart of the study.

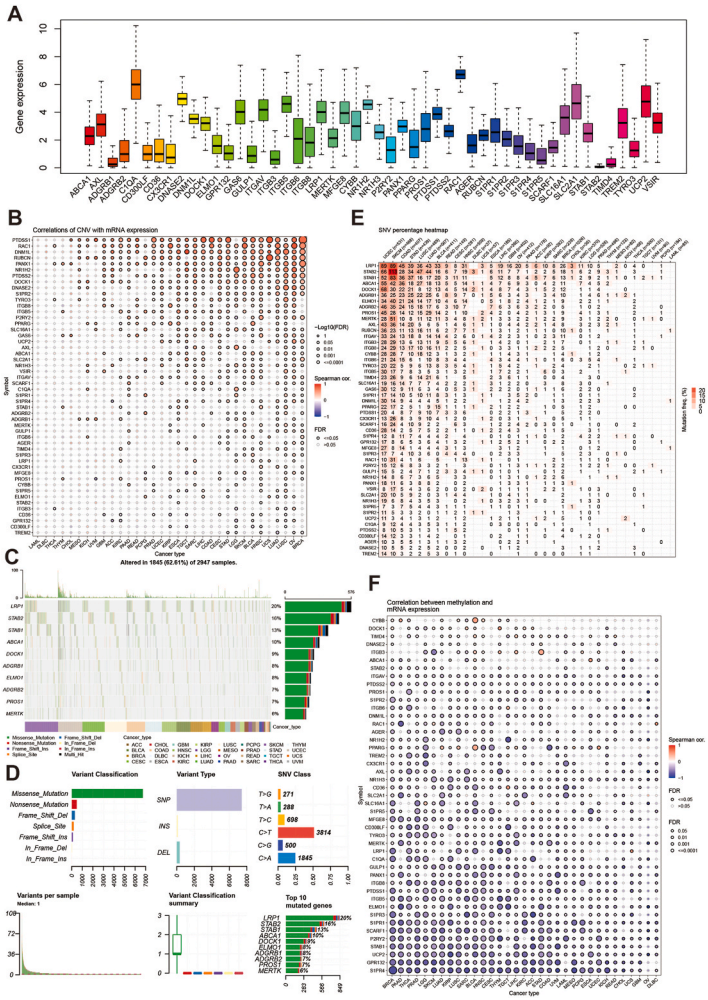

Fig. 2. Landscape of efferocytosis in pan-cancer. **(A)** Expression levels of 50 efferocytosis-related regulator genes in the cancer types. **(B)** Correlation between the CNV and regulator gene expression. **(C, D)** Alterations and variations of the regulator genes. **(E)** Heatmap showing the percentage of SNVs in the regulator genes. **(F)** Correlation between methylation and regulator gene expression.

genes encodes the type 1 receptor tyrosine kinase MerTK, which is currently being investigated in several clinical trials as a potential immune-related target for cancer intervention [29,30]. The percentage of SNVs in the regulator genes is shown in Fig. 2E. Additionally, Spearman correlation analysis revealed that DNA methylation usually correlated negatively with mRNA level (Fig. 2F), suggesting that it suppresses regulator gene expression. We also examined potential protein-protein interactions. Tight interactions were observed for merTK, BAI1, MFGE8, AXL, DOCK1, TIMD4, STAB2, GAS6, and GULP1 (Fig. S2).

3.2. Clinical relevance of the EPI in pan-cancer

To evaluate the role of efferocytosis in tumourigenesis, we used ssGSEA based on enrichment to determine the EPI (i.e. efferocytosis level) of various normal and cancer tissues. Renal clear cell carcinoma (KIRC) had the highest EPI, and acute myeloid leukaemia (LAML) had the lowest (Fig. 3A). Seven cancer types (KIRC, LAML, glioblastoma multiforme, low-grade brain glioma, ovarian serous cystadenocarcinoma, pancreatic adenocarcinoma, and testicular germ cell cancer) had significantly higher EPIs than did the corresponding normal tissues. Conversely, 17 cancer types had significantly lower EPIs than did normal tissues.

Cox regression and Kaplan–Meier survival analyses were conducted to explore the prognostic role of the EPI using OS, PFI, DSS, and DFI as clinical endpoints. The results are summarized in Fig. 3B. The EPI predicted poor OS in 18 of the 33 cancer types ($p < 0.05$) and was only favourable for lung adenocarcinoma, sarcoma, and skin cutaneous melanoma (SKCM) (Fig. 3C, S3). Additionally, the EPI significantly correlated with PFI and DSS in most cancer types, either as a good or bad prognostic biomarker (Fig. 3D and E; S4, S5), whereas the association between the EPI and DFI was significant in only a few cancer types [adrenocortical carcinoma (ACC), oesophageal carcinoma (ESCA), head and neck squamous cell carcinoma (HNSC), kidney renal papillary cell carcinoma, liver hepatocellular carcinoma, and ovarian cancer]. In a Kaplan–Meier analysis, the EPI was a risk biomarker for DFI in patients with ESCA

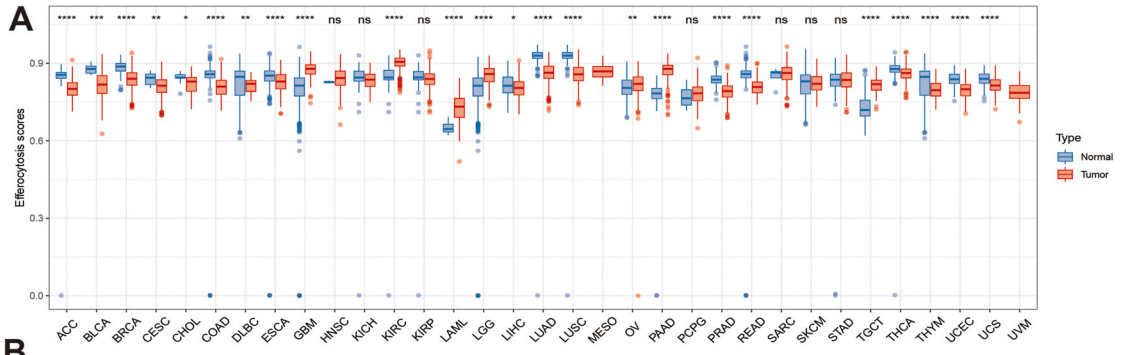

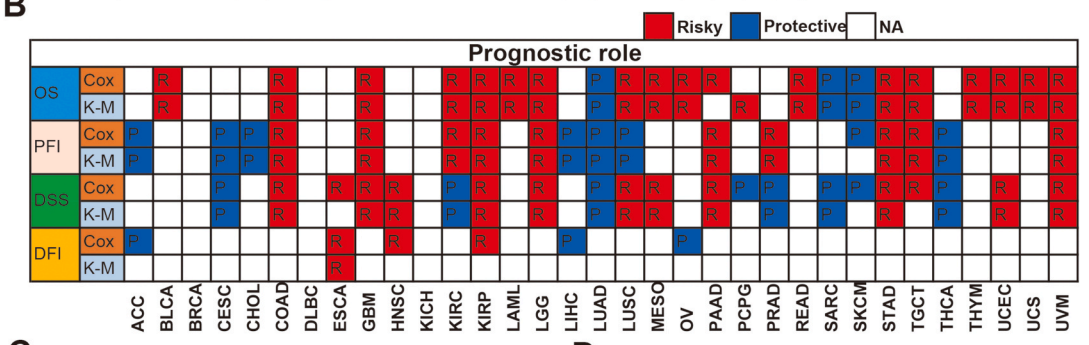

C

	pvalue	Hazard ratio
ACC	0.246	0.621(0.278−1.388)
BLCA	0.010	1.471(1.095−1.975)
BRCA	0.150	1.397(0.886−2.202)
CESC	0.074	0.566(0.304−1.056)
CHOL	0.370	2.590(0.323−20.783)
COAD	0.008	2.005(1.196−3.361)
DLBC	0.160	0.353(0.083−1.507)
ESCA	0.101	1.558(0.917−2.646)
GBM	0.039	1.485(1.019−2.162)
HNSC	0.051	1.340(0.998−1.800)
KICH	0.999	0.000(0.500−20.000)
KIRC	0.012	1.648(1.117−2.432)
KIRP	<0.001	2.859(1.555−5.256)
LAML	0.005	1.973(1.225−3.178)
LGG	0.002	1.972(1.281−3.034)
LIHC	0.125	1.313(0.927−1.860)
LUAD	0.004	0.649(0.485−0.869)
LUSC	0.001	1.688(1.234−2.308)
MESO	<0.001	2.379(1.472−3.844)
OV	0.006	1.723(1.169−2.539)
PAAD	0.002	4.920(1.792−13.510)
PCPG	0.068	0.197(0.034−1.125)
PRAD	0.118	0.338(0.087−1.317)
READ	0.012	4.071(1.357−12.216)
SARC	0.003	0.533(0.353−0.805)
SKCM	<0.001	0.577(0.439−0.757)
STAD	0.001	1.758(1.254−2.464)
TGCT	0.020	17.093(1.549−188.650)
THCA	0.126	0.462(0.171−1.244)
THYM	0.014	7.309(1.499−35.644)
UCEC	0.002	4.096(1.657−10.125)
UCS	0.046	2.776(1.016−7.581)
UVM	<0.001	7.495(2.970−18.914)

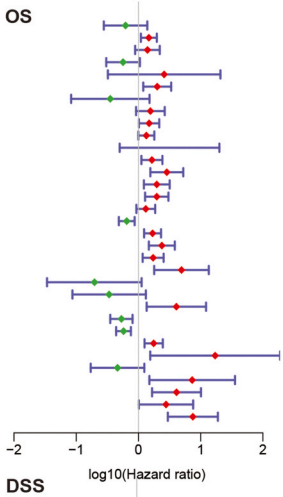

D

	pvalue	Hazard ratio
ACC	0.012	0.409(0.203−0.823)
BLCA	0.137	0.782(0.566−1.081)
BRCA	0.210	0.810(0.582−1.126)
CESC	0.010	0.464(0.258−0.832)
CHOL	0.045	0.397(0.161−0.979)
COAD	0.014	1.797(1.127−2.864)
DLBC	0.067	0.222(0.044−1.110)
ESCA	0.054	1.547(0.992−2.413)
GBM	0.003	1.755(1.212−2.544)
HNSC	0.100	0.790(0.596−1.047)
KICH	0.106	2.993(0.793−11.293)
KIRC	0.021	1.670(1.080−2.583)
KIRP	0.006	2.104(1.233−3.591)
LGG	<0.001	2.750(1.532−4.937)
LIHC	0.014	0.597(0.396−0.900)
LUAD	0.040	0.736(0.550−0.986)
LUSC	0.035	0.670(0.463−0.971)
MESO	0.112	1.540(0.905−2.623)
OV	0.382	0.886(0.676−1.162)
PAAD	<0.001	6.161(2.240−16.949)
PCPG	0.060	0.342(0.112−1.045)
PRAD	0.027	1.682(1.062−2.664)
READ	0.301	1.672(0.631−4.432)
SARC	0.135	0.773(0.552−1.083)
SKCM	0.024	0.731(0.558−0.960)
STAD	0.006	1.990(1.223−3.239)
TGCT	0.044	2.045(1.021−4.097)
THCA	0.003	0.423(0.242−0.741)
THYM	0.152	4.336(0.581−32.351)
UCEC	0.063	2.283(0.957−5.450)
UCS	0.305	1.407(0.733−2.700)
UVM	<0.001	4.167(1.904−9.122)

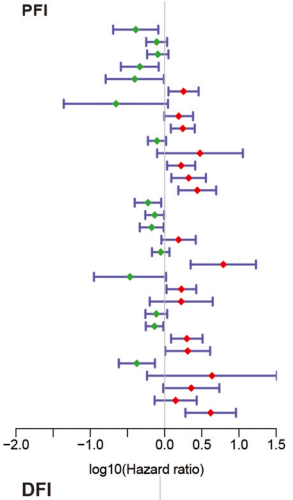

E

	pvalue	Hazard ratio
ACC	0.138	0.515(0.215−1.238)
BLCA	0.064	1.401(0.980−2.002)
BRCA	0.357	1.264(0.768−2.081)
CESC	0.019	0.451(0.232−0.876)
CHOL	0.136	3.443(0.678−17.471)
COAD	0.012	2.367(1.208−4.638)
DLBC	0.112	4.905(0.690−34.883)
ESCA	0.028	1.924(1.073−3.451)
GBM	0.022	1.586(1.070−2.350)
HNSC	0.046	1.466(1.006−2.136)
KIRC	0.035	0.626(0.405−0.969)
KIRP	<0.001	4.080(1.877−8.870)
LGG	0.002	2.074(1.313−3.276)
LIHC	0.237	0.727(0.429−1.232)
LUAD	0.003	0.567(0.391−0.823)
LUSC	0.019	1.820(1.101−3.008)
MESO	0.008	2.385(1.253−4.543)
OV	0.053	1.436(0.996−2.071)
PAAD	0.004	5.569(1.743−17.795)
PCPG	0.027	0.102(0.013−0.773)
PRAD	0.038	0.139(0.021−0.900)
SARC	0.010	0.558(0.357−0.872)
SKCM	<0.001	0.598(0.447−0.801)
STAD	0.003	2.128(1.283−3.528)
TGCT	0.020	17.093(1.549−188.650)
THCA	0.035	0.103(0.012−0.856)
UCEC	<0.001	6.206(2.387−16.133)
UCS	0.229	1.649(0.730−3.725)
UVM	<0.001	6.913(2.702−17.688)

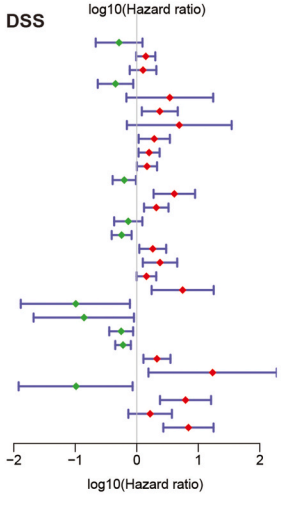

F

	pvalue	Hazard ratio
ACC	0.040	0.246(0.065−0.937)
BLCA	0.060	0.396(0.151−1.040)
BRCA	0.276	0.720(0.398−1.302)
CESC	0.055	0.385(0.145−1.020)
CHOL	0.178	0.417(0.117−1.490)
COAD	0.073	0.395(0.143−1.089)
DLBC	0.377	3.122(0.249−39.122)
ESCA	0.011	3.297(1.318−8.244)
HNSC	0.001	3.791(1.697−8.469)
KIRP	0.009	2.882(1.307−6.354)
LGG	0.061	6.831(0.914−51.060)
LIHC	0.023	0.659(0.460−0.944)
LUAD	0.084	0.675(0.432−1.055)
LUSC	0.132	0.638(0.355−1.145)
OV	0.020	0.663(0.469−0.937)
PCPG	0.139	5.638(0.570−55.758)
PRAD	0.100	0.548(0.268−1.121)
READ	0.174	3.620(0.567−23.125)
SARC	0.099	0.657(0.398−1.082)
STAD	0.059	3.914(0.947−16.171)
TGCT	0.086	5.801(0.782−43.061)
THCA	0.109	0.450(0.170−1.194)
UCEC	0.078	0.363(0.118−1.119)

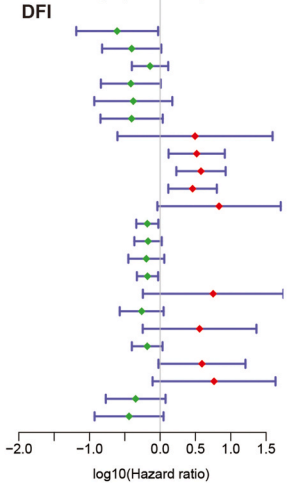

(caption on next page)

Fig. 3. Clinical relevance of the EPI in cancer. **(A)** EPIs in cancer and corresponding normal tissues. **(B)** Summary of the correlations between the EPI and prognosis outcome in the cancer types. **(C–F)** Forest plots showing the correlation of the EPI with OS, PFI, DSS, and DFI in the cancer types.

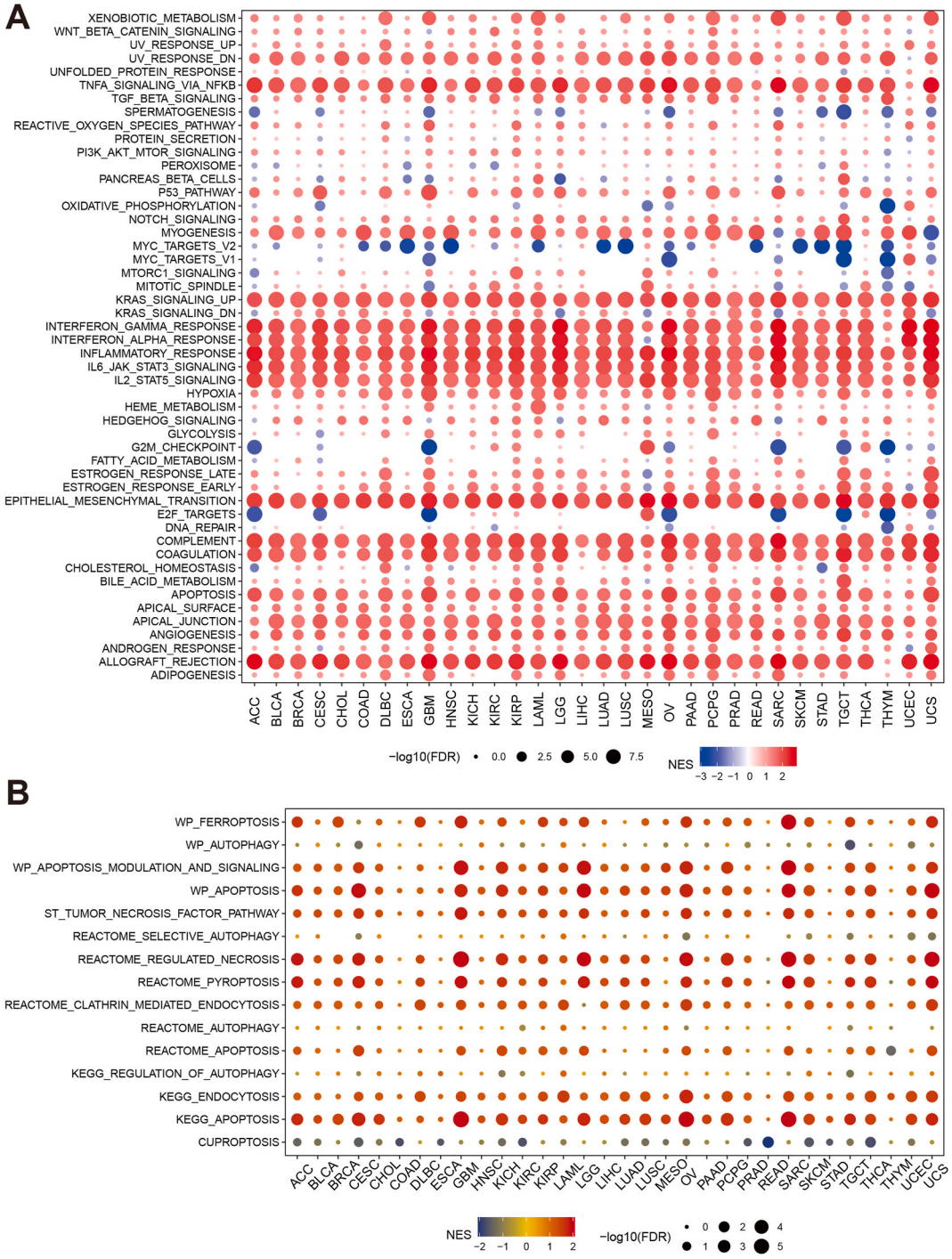

Fig. 4. Association of the EPI with signalling pathways and biological behaviour in pan-cancer. **(A)** Signalling pathways. **(B)** Cell death-related pathways.

(Fig. S6).

3.3. The EPI and signalling pathways in pan-cancer

We investigated the connection between efferocytosis level and signalling pathways in the 33 cancers via GSEA based on normalised enrichment scores [31]. Several immune-related pathways were screened for involvement of efferocytosis-related regulator genes; these pathways included the complement, IL-6/JAK/STAT3, IL-2/JAK/STAT55, and tumour necrosis α (TNFα)-activated NF-κB pathways and those mediating interferon α, γ, and inflammatory responses and allograft rejection (Fig. 4A).

Considering the role of efferocytosis in clearing ACs, we also examined the association between the EPI and cell death-related pathways. We found that apoptosis and necrosis pathways were enriched in most cancer types, whereas enrichment of the autophagy pathway was seldom observed (Fig. 4B).

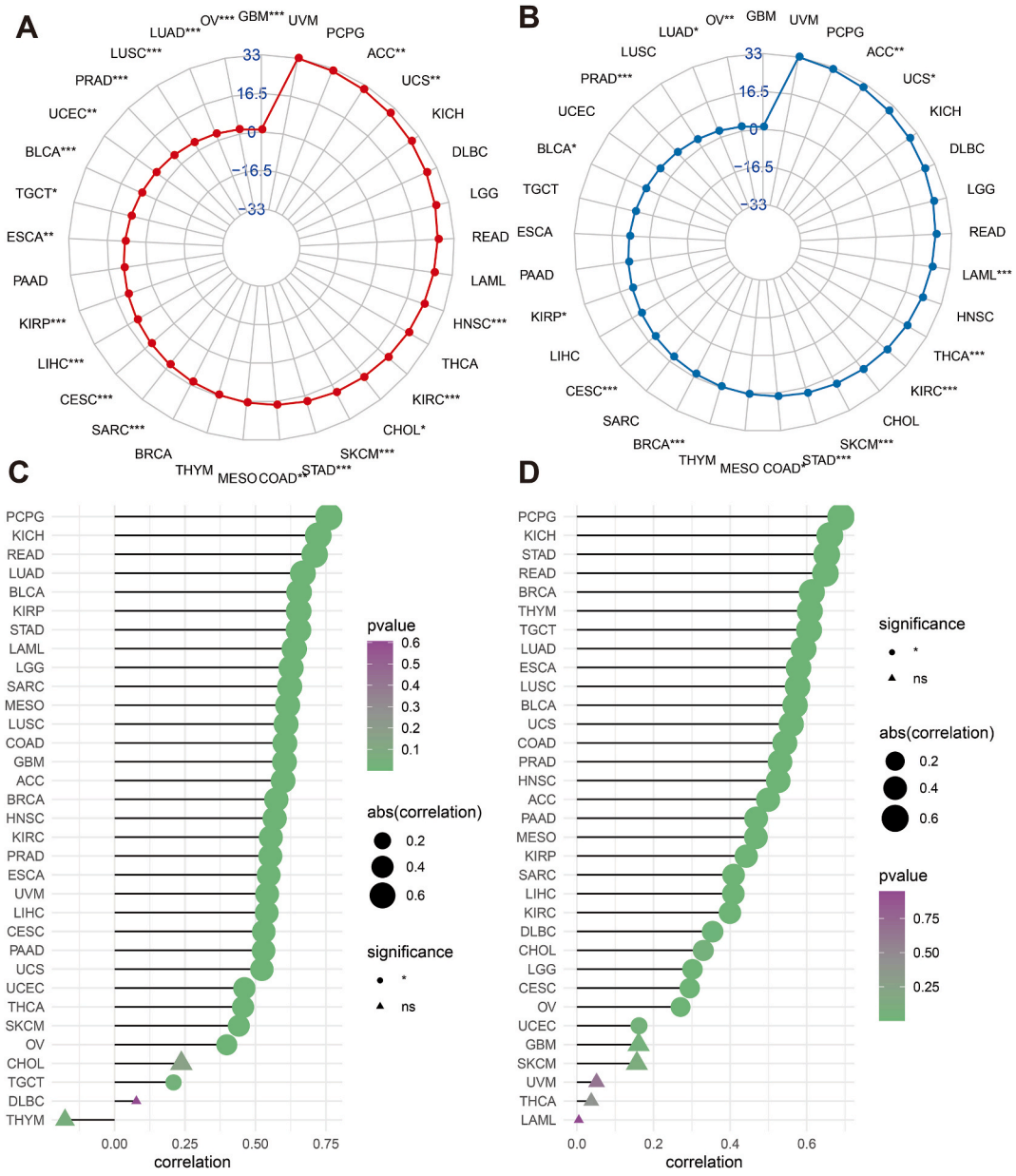

Fig. 5. Association between the EPI and molecular features. The molecular features were TMB **(A)**, MSI **(B)** ESTIMATE score **(C)**, and stromal score **(D)**.

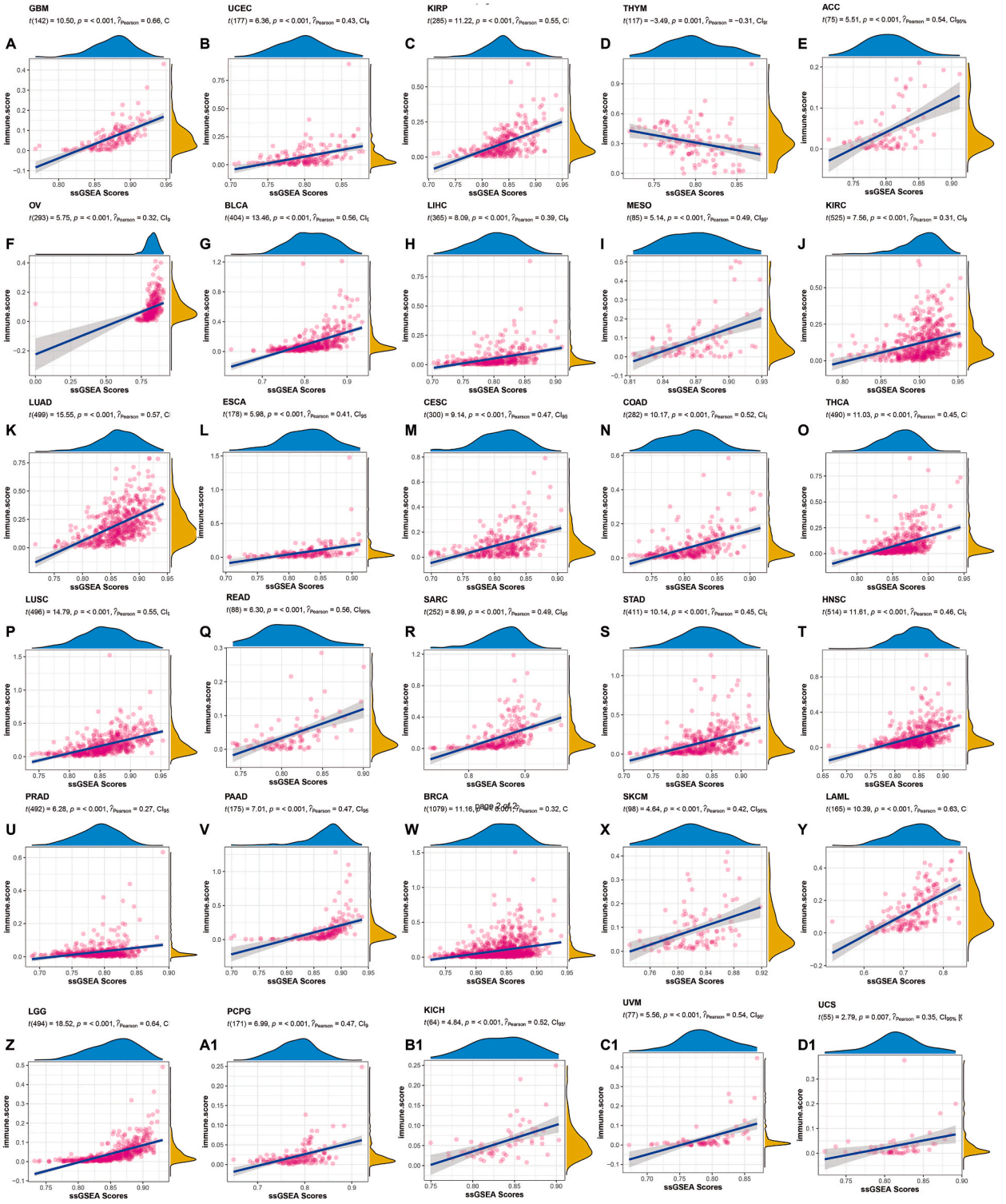

Fig. 6. Association between the EPI and immune score in the cancer types. **(A)** GBM, **(B)** UCEC. **(C)** KIRP. **(D)**THYM. **(E)** ACC. **(F)** OV. **(G)** BLCA. **(H)** LIHC. **(I)** MESO. **(J)** KIRC. **(K)** LUAD. **(L)** ESCA. **(M)** CESC. **(N)** COAD. **(O)**THCA. **(P)** LUSC. **(Q)**READ. **(R)**SARC. **(S)**STAD. **(T)**HNSC. **(U)**PRAD. **(V)**PAAD. **(W)**BRCA. **(X)**SKCM. **(Y)** LAML. **(Z)** LGG. **(A1)** PCPG. **(B1)** KICH. **(C1)** UVM. **(D1)** UCS.

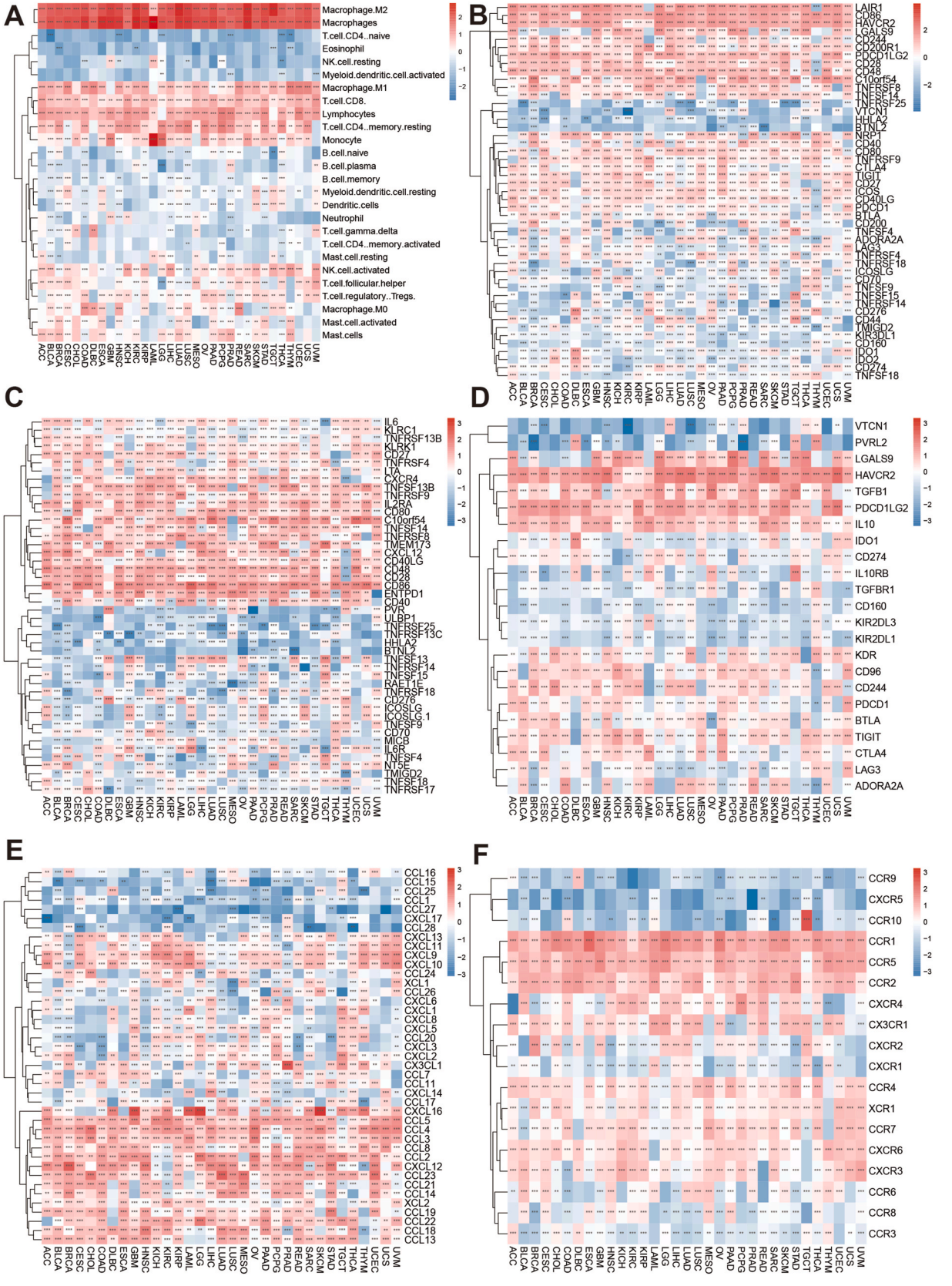

(caption on next page)

Fig. 7. Association between the EPI and immune status. The immune status parameters were immune cell infiltration level **(A)**, immune checkpoint **(B)**, immunostimulatory **(C)**, immunosuppressive, **(D)** chemokine **(E)**, and chemokine receptor **(F)** genes.

3.4. The EPI and immune infiltration

Efferocytosis likely promotes tumour development by creating an immunosuppressive tumour environment via dead cell clearance [32]. Understanding the connection between efferocytosis and immunologic regulation in the TME would aid the design of better therapeutic regimens, especially those including immunotherapy.

First, we analysed the relevance of the EPI to TMB and MSI. Both TMB and MSI predict immunotherapy responses in some cancers, with higher TMB and MSI levels indicating better responses [33,34]. Our analysis showed a significant positive correlation between the EPI and TMB in ACC, uterine carcinosarcoma (UCS), HNSC, KIRC, cholangiocarcinoma, SKCM, stomach adenocarcinoma (STAD), and colon adenocarcinoma (COAD) (Fig. 5A), and between the EPI and MSI in ACC, UCS, LAML, thyroid carcinoma, KIRC, SKCM, STAD,

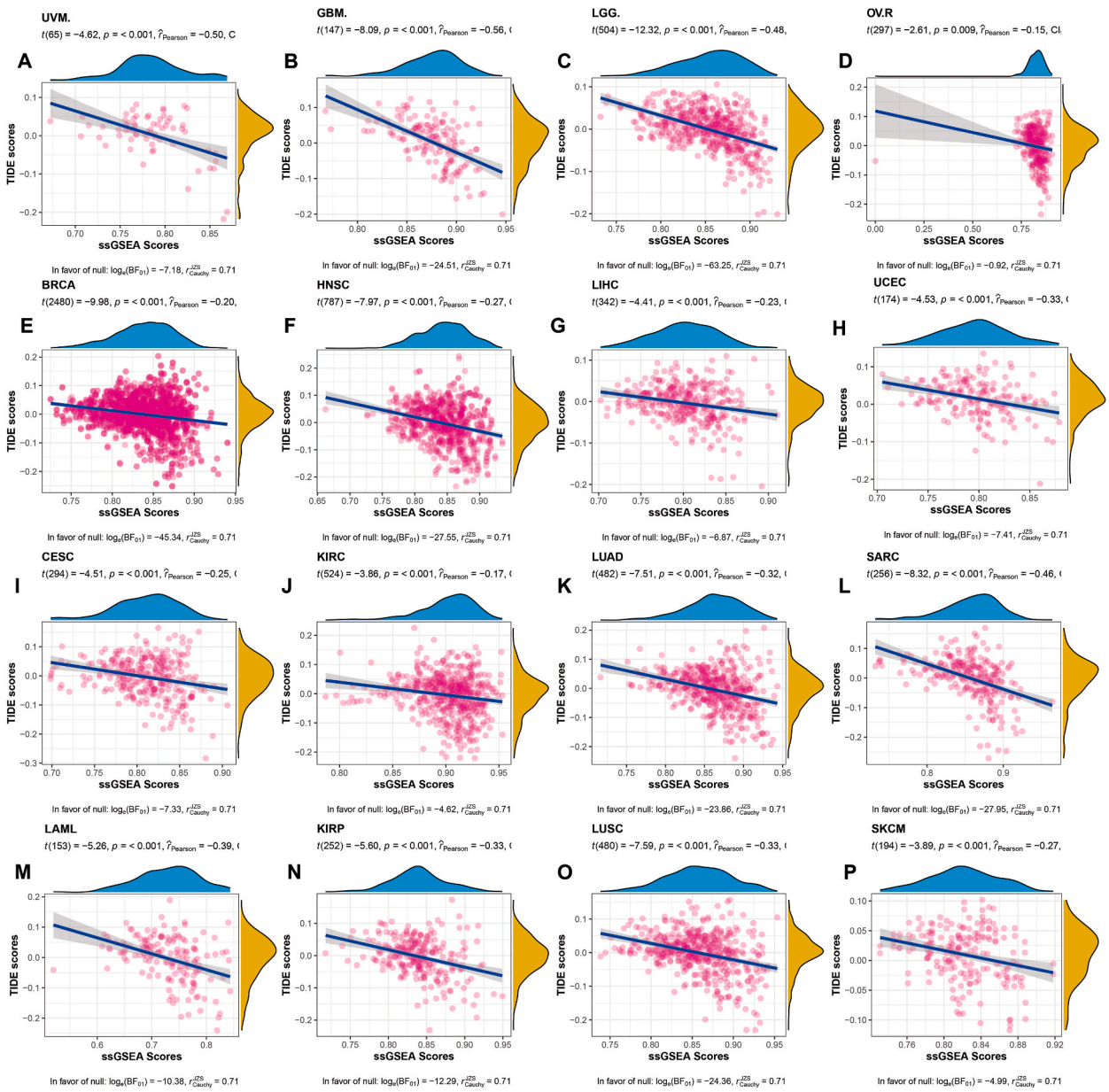

Fig. 8. Association between the EPI and TIDE score in the cancer types. **(A) UVM. (B)** GBM. **(C)** LGG. **(D)** OV. **(E)** BRCA. **(F)** HNSC. **(G)** LIHC. **(H)** UCEC. **(I)** CESC. **(J)** KIRC. **(K)** LUAD. **(L)** SARC. **(M)** LAML. **(N)** KIRP. **(O)** LUSC. **(P)** SKCM.

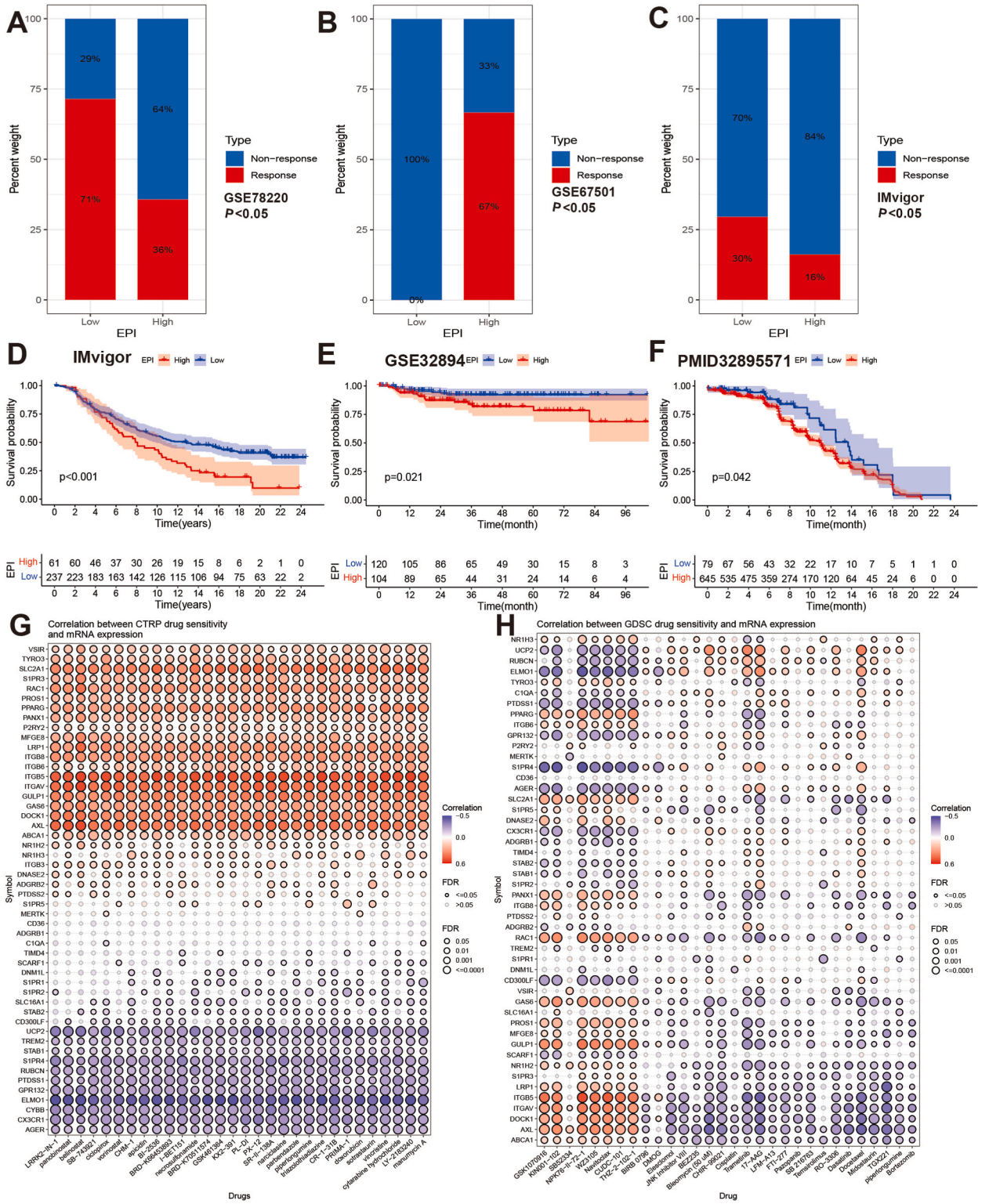

Fig. 9. Association between the EPI and cancer treatment. Associations of the EPI with immunotherapy responses **(A–C)**, prognosis of immunotherapy recipients **(D–F)**, and drug sensitivity **(G, H)** are shown.

and COAD (Fig. 5B).

Second, we assessed the association of the EPI with ESTIMATE, stromal, and immune scores using the ESTIMATE algorithm. The EPI positively correlated with ESTIMATE (Fig. 5C) and stromal (Fig. 5D) scores in most cancer types. Indicative of immune cell infiltration of the tumour, it also positively correlated with the immune score in 29 of the 33 cancer types (Fig. 6A-6D1); a negative correlation was only observed for mesothelioma.

As determined via Spearman correlation coefficient analysis, the EPI was associated with a specific type of immune cell infiltration (Fig. 7A). Notably, it positively correlated with macrophage, especially M2 macrophage, infiltration in all cancer types. M2 macrophages are mainly involved in anti-inflammatory responses [35]. There was also a positive association between the EPI and M1 macrophage, $CD8^+$ T cell, lymphocyte, $CD4^+$ memory T cell, and monocyte infiltration.We also examined the association between the EPI and the expression of immune checkpoint (Fig. 7B), immunostimulatory (Fig. 7C), immunosuppressive (Fig. 7D), MHC (Fig. S7), chemokine (Fig. 7E), and chemokine receptor (Fig. 7F, S7) genes. Both positive and negative correlations were observed. The EPI positively correlated with the mRNA expression of *HAVCR2* (all cancer types), *LAIR1* and *CD86* (nearly all cancer types), and the genes encoding CCL5 and its receptor (most cancer types). TIM-3, the protein product of *HAVCR2*, is a promising immune checkpoint target [36]. Leukocyte-associated immunoglobulin-like receptors (LAIRS, encoded by *LAIR1*) are expressed on most immune cell types, and blockade of LAIR1 signalling has been shown to inhibit tumour development [36]. The CCL5/CCR5 axis facilitates tumour progression, and several anti-CCR5 clinical trials are currently underway [37].

3.5. The EPI and treatment

Efferocytosis tends to promote immune tolerance that can be used by cancer cells for their expansion; as such, it might directly influence the immunotherapy response. Therefore, we analysed the association between the EPI and TIDE score. A higher TIDE score indicates better tumour immune escape and a lower immunotherapy response. Significant negative correlations between the EPI and TIDE score were observed in 16 cancer types (Fig. 8A-8P).

We also explored the association between the EPI and immune response in patients receiving immunotherapy as part of their cancer treatment. Among patients with melanoma (GSE78220 cohort) who received anti-programmed cell death protein (PD-1) therapy, 71 % in the low EPI group had an immune response compared with only 36 % in the high EPI group (Fig. 9A). Among similarly treated patients with renal cell carcinoma (RCC), 67 % in the high EPI group (GSE67501 cohort) had an immune response (Fig. 9B), whereas no patients in the low EPI group had an immune response. Among patients in the IMvigor210 clinical trial for urothelial cancer (UC), 30 % and 16 % in the low and high EPI groups had an immune response, respectively (Fig. 9C). Despite the inconsistent relationship between EPI and immunotherapy response in the different cancers, our survival analysis showed that lower EPI corelated with longer OS time in patients with UC (IMvigor210, GSE32894 cohorts; Fig. 9D and E) and those with advanced RCC (PMID: 32895571 cohort, Fig. 9F).

3.6. Efferocytosis-related regulator gene expression and drug sensitivity

To further clarify the function of EPI in cancer treatment, we analysed the association between efferocytosis-related regulator gene expression and drug sensitivity using the CTRP and GDSC datasets. We selected the 30 compounds ($|r| > 0.3$) that most likely targeted these genes. The mRNA levels of nearly 20 genes positively correlated with sensitivity to all 30 cancer drugs. Those of 11 genes negatively correlated with sensitivity to drugs in the CTRP dataset (Fig. 9G), whereas both positive and negative correlations were observed for drugs in the GDSC dataset (Fig. 9H).

Several efferocytosis-related proteins have been identified as potential cancer treatment targets. These include the TAM receptor tyrosine kinases (Tyro3, Axl and MerTK), which mediate immune regulation in the TME and are overexpressed in cancer. The combination of TAM receptor targeting and conventional therapy may improve therapeutical efficiency [38]. In our study, the mRNA levels of the genes encoding Tyro3 and Axl levels positively correlated with sensitivity to most of the 30 drugs; whether those of MerTK did so as well was unclear.

4. Discussion

Efferocytosis is essential for maintaining homeostasis. Previous studies have shown that defective efferocytosis leads to cancer and inflammatory, autoimmune, and other diseases [39,40]. Efferocytosis is executed by “professional” phagocytes (e.g. macrophages, dendritic cells) and “non-professional” phagocytes (epithelial cells) [41]. Exploring the mechanistic basis of cell clearance by phagocytes would help us understand why these diseases occur and progress.

The tumour mass consists not only of cancer cells but also of the immune cells, macrophages, and extracellular matrix in the TME [42]. In certain solid cancers, infiltrating macrophages account for almost 50 % of the tumour mass [43]. M2-polarized tumour--associated macrophages formed in the TME create an anti-inflammatory environment that facilitates tumour development and promotes drug resistance. Several therapeutic targets (such as macrophage TAM receptors) have been identified. To uncover additional targets, we analysed the mRNA expression of 50 efferocytosis-related regulator genes in 33 cancer types; we found that *C1QA* and *RAC1* were highly expressed. Complement C1q A chain (C1QA) is a marker of TME remodelling in osteosarcoma and an immune-related marker in skin cutaneous melanoma [44,45]. C1Q-positive tumour-associated macrophages promote T cell exhaustion and thus likely drive tumour growth [46]. The GTPase Rac1 regulates cytoskeletal organisation and is frequently overexpressed in cancer cells [47,48]. More studies are needed to characterize the biological functions of these two proteins in cancer.

In this study, we established an EPI model to describe the efferocytosis levels of different cancers and corresponding normal tissues. KIRC had the highest EPI, and LAML had the lowest EPI. As evidence of the complexity of the relationship between efferocytosis and cancer, both elevated and reduced efferocytosis levels were observed in tumour vs. normal tissues.

We found that the EPI correlated with immune-associated pathway enrichment in all cancer types; the enriched pathways included the complement, IL-6/JAK/STAT3, IL-2/JAK/STAT55, and TNFα-activated NF-κB pathways and those mediating interferon α, γ, and inflammatory responses and allograft rejection. Although the function of the TNF family members in cancer progression has been elaborated, the relationship of TNFα signalling to and its targets in efferocytosis remains unclear [49].

In our study, the EPI positively correlated with the expression of three immune-related genes in all 33 cancer types: *HAVCR2*, *LAIR1*, and *CD86*, which encode TIM-3, LAIR1, and CD86, respectively. TIM-3 mediates immune suppression and has been extensively discussed [50–52]. In patients with PD-1-treated melanoma, collagen, LAIR1, and TIM-3 were overexpressed and predicted poor survival and immunotherapy responses [53]. In the study by Xie et al., an anti-LAIR1 monoclonal antibody inhibited the activity of immunosuppressive myeloid cells and reactivated T cells from cancer patients *in vitro* [54]. However, more experiments are needed to validate the role of LAIR1 in cancer immunotherapy. CD86 regulates T cell responses by binding to CD28 or CTLA-1 [55]. Julia et al. designed a therapeutic strategy to prevent severe COVID-19; this strategy involved targeting the CD80/86 pro-inflammatory axis using abatacept, a selective stimulation modulator [56].

In our Cox regression and Kaplan–Meier survival analyses, the EPI tended to be a prognostic risk factor for OS in most cancer types. We also found that the EPI significantly and negatively correlated with the TIDE score in 16 cancer types. Higher TIDE scores usually indicate weaker immunotherapy responses. However, analysis of distinct immunotherapy-treated cancers showed an inconsistent correlation; we speculate that this may reflect limited sample size. Nevertheless, lower EPI corelated with longer OS time in immunotherapy-treated patients with UC (IMvigor210, GSE32894 cohorts) or advanced RCC (PMID: 32895571 cohort) in our survival analyses.

To potentially match gene expression profiles with medical regimens, we examined the relationship between the EPI and drug sensitivity using the CTRP and GDSC datasets. We found that expression of the genes encoding Tyro3 and Axl positively correlated with sensitivity to most of the compounds tested.

Efferocytosis is essential for accurate removal of dead cells and health maintenance. It is a complicated procedure accomplished by the coordinated actions of phagocytes and ACs. To date, the mechanisms underlying efferocytosis are not fully understood. Our selection of efferocytosis-related regulator genes was based on previous studies and may be incomplete; moreover, some regulator genes have other functions. This may have limited the accuracy and sensitivity of our EPI model. In addition, the significant negative correlation between the EPI and TIDE score in 16 cancer types was inconsistent with the results of our survival analysis of the GSE78220 (melanoma), GSE67501 (RCC), and IMvigor210 (UC) cohorts, perhaps owing to insufficient sample size. We believe future research and new discoveries regarding efferocytosis will improve the precision and sensitivity of our EPI model.

5. Conclusions

Our study systematically analysed the expression profiles and variations of 50 efferocytosis-related regulator genes in 33 cancer types. To represent efferocytosis levels, we established an EPI model based on enrichment scores. We examined the relationship of the EPI to immune-related molecules and pathways and clinical outcomes. The expression of *HAVCR2*, *LAIR1*, and *CD86* positively correlated with the EPI in all cancer types. Further studies are needed to fully uncover the mechanisms underlying efferocytosis, toward the goal of providing better therapeutic options with stronger immune responses.

Ethical approval

The ethical approval is not applicable because these data is from public data platform.

Funding

This study was supported by Hunan Provincial Natural Science Foundation of China (Grant No.2023JJ30907).

Data availability statement

The data can be available from the public database (TCGA: (https://portal.gdc.cancer.gov).

CRediT authorship contribution statement

Peng Chen: Writing – original draft, Data curation. **Zhanzhan Li:** Software, Methodology, Formal analysis. **Na Li:** Writing – review & editing, Visualization, Supervision, Data curation.

Declaration of competing interest

The authors declare that they have no known competing financial interests or personal relationships that could have appeared to influence the work reported in this paper.

Appendix A. Supplementary data

Supplementary data to this article can be found online at https://doi.org/10.1016/j.heliyon.2024.e30337.

References

[1] R. Sender, R. Milo, The distribution of cellular turnover in the human body, Nat. Med. 27 (2021) 45–48. https://10.1038/s41591-020-01182-9.
[2] A.C. Doran, A.J. Yurdagul, I. Tabas, Efferocytosis in health and disease, Nat. Rev. Immunol. 20 (2020) 254–267. https://10.1038/s41577-019-0240-6.
[3] E. Boada-Romero, J. Martinez, B.L. Heckmann, D.R. Green, The clearance of dead cells by efferocytosis, Nat. Rev. Mol. Cell Biol. 21 (2020) 398–414. https://10.1038/s41580-020-0232-1.
[4] M.T. Silva, Secondary necrosis: the natural outcome of the complete apoptotic program, FEBS Lett. 584 (2010) 4491–4499. https://10.1016/j.febslet.2010.10.046.
[5] P. Mehrotra, K.S. Ravichandran, Drugging the efferocytosis process: concepts and opportunities, Nat. Rev. Drug Discov. 21 (2022) 601–620. https://10.1038/s41573-022-00470-y.
[6] K.S. Ravichandran, Beginnings of a good apoptotic meal: the find-me and eat-me signaling pathways, Immunity 35 (2011) 445–455. https://10.1016/j.immuni.2011.09.004.
[7] S. Nagata, J. Suzuki, K. Segawa, T. Fujii, Exposure of phosphatidylserine on the cell surface, Cell Death Differ. 23 (2016) 952–961. https://10.1038/cdd.2016.7.
[8] C.A. Bradley, CD24 - a novel 'don't eat me' signal, Nat. Rev. Drug Discov. 18 (2019) 747. https://10.1038/d41573-019-00146-0.
[9] E. Boada-Romero, J. Martinez, B.L. Heckmann, D.R. Green, The clearance of dead cells by efferocytosis, Nat. Rev. Mol. Cell Biol. 21 (2020) 398–414. https://10.1038/s41580-020-0232-1.
[10] D. Hanahan, R.A. Weinberg, Hallmarks of cancer: the next generation, Cell 144 (2011) 646–674. https://10.1016/j.cell.2011.02.013.
[11] A. Tajbakhsh, H.S. Gheibi, A. Movahedpour, A. Savardashtaki, R. Loveless, G.E. Barreto, Y. Teng, A. Sahebkar, The complex roles of efferocytosis in cancer development, metastasis, and treatment, Biomed. Pharmacother. 140 (2021) 111776. https://10.1016/j.biopha.2021.111776.
[12] Y. Zhou, Y. Yao, Y. Deng, A. Shao, Regulation of efferocytosis as a novel cancer therapy, Cell Commun. Signal. 18 (2020) 71. https://10.1186/s12964-020-00542-9.
[13] N.A. Giraldo, R. Sanchez-Salas, J.D. Peske, Y. Vano, E. Becht, F. Petitprez, P. Validire, A. Ingels, X. Cathelineau, W.H. Fridman, C. Sautes-Fridman, The clinical role of the TME in solid cancer, Br. J. Cancer 120 (2019) 45–53. https://10.1038/s41416-018-0327-z.
[14] P. Mehrotra, K.S. Ravichandran, Drugging the efferocytosis process: concepts and opportunities, Nat. Rev. Drug Discov. 21 (2022) 601–620. https://10.1038/s41573-022-00470-y.
[15] J. Zhou, Z. Tang, S. Gao, C. Li, Y. Feng, X. Zhou, Tumor-associated macrophages: recent insights and therapies, Front. Oncol. 10 (2020) 188. https://10.3389/fonc.2020.00188.
[16] M. Yang, J. Liu, C. Piao, J. Shao, J. Du, ICAM-1 suppresses tumor metastasis by inhibiting macrophage M2 polarization through blockade of efferocytosis, Cell Death Dis. 6 (2015) e1780. https://10.1038/cddis.2015.144.
[17] K.V. Myers, S.R. Amend, K.J. Pienta, Targeting Tyro3, Axl and MerTK (TAM receptors): implications for macrophages in the tumor microenvironment, Mol. Cancer 18 (2019) 94. https://10.1186/s12943-019-1022-2.
[18] Y. Duan, W. Wong, S.C. Chua, H.L. Wee, S.G. Lim, B.T. Chua, H.K. Ho, Overexpression of Tyro3 and its implications on hepatocellular carcinoma progression, Int. J. Oncol. 48 (2016) 358–366. https://10.3892/ijo.2015.3244.
[19] Z.T. Chai, X.P. Zhang, J.Y. Ao, X.D. Zhu, M.C. Wu, W.Y. Lau, H.C. Sun, S.Q. Cheng, AXL overexpression in tumor-derived endothelial cells promotes vessel metastasis in patients with hepatocellular carcinoma, Front. Oncol. 11 (2021) 650963. https://10.3389/fonc.2021.650963.
[20] X. Shao, Y. Sun, K. Zhong, J. Gu, Y. Yu, T. Hu, X. Kuai, Y. Xing, TYRO3 promotes tumorigenesis and drug resistance in colorectal cancer by enhancing the epithelial-mesenchymal transition process, Aging (Albany NY) 15 (2023) 3035–3051. https://10.18632/aging.204656.
[21] X. Qu, J. Liu, X. Zhong, X. Li, Q. Zhang, Role of AXL expression in non-small cell lung cancer, Oncol. Lett. 12 (2016) 5085–5091. https://10.3892/ol.2016.5356.
[22] J. Schlegel, M.J. Sambade, S. Sather, S.J. Moschos, A.C. Tan, A. Winges, D. Deryckere, C.C. Carson, D.G. Trembath, J.J. Tentler, S.G. Eckhardt, P.F. Kuan, R. L. Hamilton, L.M. Duncan, C.R. Miller, N. Nikolaishvili-Feinberg, B.R. Midkiff, J. Liu, W. Zhang, C. Yang, X. Wang, S.V. Frye, H.S. Earp, J.M. Shields, D. K. Graham, MERTK receptor tyrosine kinase is a therapeutic target in melanoma, J. Clin. Invest. 123 (2013) 2257–2267. https://10.1172/JCI67816.
[23] J.H. Yi, J. Jang, J. Cho, I.G. Do, M. Hong, S.T. Kim, K.M. Kim, S. Lee, S.H. Park, J.O. Park, Y.S. Park, W.K. Kang, H.Y. Lim, J. Lee, MerTK is a novel therapeutic target in gastric cancer, Oncotarget 8 (2017) 96656–96667. https://10.18632/oncotarget.3750.
[24] Qian Bi, Xin Lian, Jing Shen, F. Zhang, T. Xu, Exploration of radiotherapy strategy for brain metastasis patients with driver gene positivity in lung cancer, J. Cancer 15 (2024) 1994–2002.
[25] D. Korns, S.C. Frasch, R. Fernandez-Boyanapalli, P.M. Henson, D.L. Bratton, Modulation of macrophage efferocytosis in inflammation, Front. Immunol. 2 (2011) 57. https://10.3389/fimmu.2011.00057.
[26] S. Morioka, C. Maueroder, K.S. Ravichandran, Living on the edge: efferocytosis at the interface of homeostasis and pathology, Immunity 50 (2019) 1149–1162. https://10.1016/j.immuni.2019.04.018.
[27] K. Yoshihara, M. Shahmoradgoli, E. Martinez, R. Vegesna, H. Kim, W. Torres-Garcia, V. Trevino, H. Shen, P.W. Laird, D.A. Levine, S.L. Carter, G. Getz, K. Stemke-Hale, G.B. Mills, R.G. Verhaak, Inferring tumour purity and stromal and immune cell admixture from expression data, Nat. Commun. 4 (2013) 2612. https://10.1038/ncomms3612.
[28] X. Shao, N. Lv, J. Liao, J. Long, R. Xue, N. Ai, D. Xu, X. Fan, Copy number variation is highly correlated with differential gene expression: a pan-cancer study, BMC Med. Genet. 20 (2019) 175. https://10.1186/s12881-019-0909-5.
[29] J.M. Huelse, D.M. Fridlyand, S. Earp, D. Deryckere, D.K. Graham, MERTK in cancer therapy: targeting the receptor tyrosine kinase in tumor cells and the immune system, Pharmacol. Ther. 213 (2020) 107577. https://10.1016/j.pharmthera.2020.107577.
[30] K.C. Lahey, V. Gadiyar, A. Hill, S. Desind, Z. Wang, V. Davra, R. Patel, A. Zaman, D. Calianese, R.B. Birge, Mertk: an emerging target in cancer biology and immuno-oncology, Int Rev Cell Mol Biol 368 (2022) 35–59. https://10.1016/bs.ircmb.2022.04.004.
[31] J. Reimand, R. Isserlin, V. Voisin, M. Kucera, C. Tannus-Lopes, A. Rostamianfar, L. Wadi, M. Meyer, J. Wong, C. Xu, D. Merico, G.D. Bader, Pathway enrichment analysis and visualization of omics data using g:Profiler, GSEA, Cytoscape and EnrichmentMap, Nat. Protoc. 14 (2019) 482–517. https://10.1038/s41596-018-0103-9.
[32] H.S. Gheibi, V. Bianconi, M. Pirro, A. Sahebkar, Efferocytosis: molecular mechanisms and pathophysiological perspectives, Immunol. Cell Biol. 97 (2019) 124–133. https://10.1111/imcb.12206.
[33] J.H. Strickler, B.A. Hanks, M. Khasraw, Tumor mutational burden as a predictor of immunotherapy response: is more always better? Clin. Cancer Res. 27 (2021) 1236–1241. https://10.1158/1078-0432.CCR-20-3054.
[34] K. Li, H. Luo, L. Huang, H. Luo, X. Zhu, Microsatellite instability: a review of what the oncologist should know, Cancer Cell Int. 20 (2020) 16. https://10.1186/s12935-019-1091-8.
[35] C. Yunna, H. Mengru, W. Lei, C. Weidong, Macrophage M1/M2 polarization, Eur. J. Pharmacol. 877 (2020) 173090. https://10.1016/j.ejphar.2020.173090.
[36] H. Li, D. Yang, M. Hao, H. Liu, Differential expression of HAVCR2 gene in pan-cancer: a potential biomarker for survival and immunotherapy, Front. Genet. 13 (2022) 972664. https://10.3389/fgene.2022.972664.
[37] Z. Zeng, T. Lan, Y. Wei, X. Wei, CCL5/CCR5 axis in human diseases and related treatments, Genes Dis 9 (2022) 12–27. https://10.1016/j.gendis.2021.08.004.

[38] A. Tajbakhsh, H.S. Gheibi, A. Movahedpour, A. Savardashtaki, R. Loveless, G.E. Barreto, Y. Teng, A. Sahebkar, The complex roles of efferocytosis in cancer development, metastasis, and treatment, Biomed. Pharmacother. 140 (2021) 111776. https://10.1016/j.biopha.2021.111776.
[39] A.C. Doran, A.J. Yurdagul, I. Tabas, Efferocytosis in health and disease, Nat. Rev. Immunol. 20 (2020) 254–267. https://10.1038/s41577-019-0240-6.
[40] Q. Bi, Z. Miao, J. Shen, H. Wang, K. Kang, J. Du, F. Zhang, S. Fan, Detecting the research trends and hot spots in external irradiation therapy for rectal cancer, J. Cancer 13 (2022) 2179–2188. https://10.7150/jca.69669.
[41] E. Boada-Romero, J. Martinez, B.L. Heckmann, D.R. Green, The clearance of dead cells by efferocytosis, Nat. Rev. Mol. Cell Biol. 21 (2020) 398–414. https://10.1038/s41580-020-0232-1.
[42] F.P. Ribeiro, A.P. Rodrigues, L.B. de Menezes, M.M. Pacheco, Tumor microenvironment components: allies of cancer progression, Pathol. Res. Pract. 216 (2020) 152729. https://10.1016/j.prp.2019.152729.
[43] N.M. Anderson, M.C. Simon, The tumor microenvironment, Curr. Biol. 30 (2020) R921–R925. https://10.1016/j.cub.2020.06.081.
[44] L.H. Chen, J.F. Liu, Y. Lu, X.Y. He, C. Zhang, H.H. Zhou, Complement C1q (C1qA, C1qB, and C1qC) may Be a potential prognostic factor and an index of tumor microenvironment remodeling in osteosarcoma, Front. Oncol. 11 (2021) 642144. https://10.3389/fonc.2021.642144.
[45] Z. Liang, L. Pan, J. Shi, L. Zhang, C1QA, C1QB, and GZMB are novel prognostic biomarkers of skin cutaneous melanoma relating tumor microenvironment, Sci. Rep. 12 (2022) 20460. https://10.1038/s41598-022-24353-9.
[46] M. Revel, C. Sautes-Fridman, W.H. Fridman, L.T. Roumenina, C1q+ macrophages: passengers or drivers of cancer progression, Trends Cancer 8 (2022) 517–526. https://10.1016/j.trecan.2022.02.006.
[47] C. Bailly, J. Beignet, G. Loirand, V. Sauzeau, Rac1 as a therapeutic anticancer target: promises and limitations, Biochem. Pharmacol. 203 (2022) 115180. https://10.1016/j.bcp.2022.115180.
[48] J. Liang, L. Oyang, S. Rao, Y. Han, X. Luo, P. Yi, J. Lin, L. Xia, J. Hu, S. Tan, L. Tang, Q. Pan, Y. Tang, Y. Zhou, Q. Liao, Rac1, A potential target for tumor therapy, Front. Oncol. 11 (2021) 674426. https://10.3389/fonc.2021.674426.
[49] D. Lin, X. Kang, L. Shen, S. Tu, C. Lenahan, Y. Chen, X. Wang, A. Shao, Efferocytosis and its associated cytokines: a light on non-tumor and tumor diseases? Mol Ther Oncolytics 17 (2020) 394–407. https://10.1016/j.omto.2020.04.010.
[50] W. Du, M. Yang, A. Turner, C. Xu, R.L. Ferris, J. Huang, L.P. Kane, B. Lu, TIM-3 as a target for cancer immunotherapy and mechanisms of action, Int. J. Mol. Sci. 18 (2017). https://10.3390/ijms18030645.
[51] Y. Wolf, A.C. Anderson, V.K. Kuchroo, TIM3 comes of age as an inhibitory receptor, Nat. Rev. Immunol. 20 (2020) 173–185. https://10.1038/s41577-019-0224-6.
[52] L. Zhao, S. Cheng, L. Fan, B. Zhang, S. Xu, TIM-3: an update on immunotherapy, Int. Immunopharm. 99 (2021) 107933. https://10.1016/j.intimp.2021.107933.
[53] D.H. Peng, B.L. Rodriguez, L. Diao, L. Chen, J. Wang, L.A. Byers, Y. Wei, H.A. Chapman, M. Yamauchi, C. Behrens, G. Raso, L. Soto, E. Cuentes, I.I. Wistuba, J. M. Kurie, D.L. Gibbons, Collagen promotes anti-PD-1/PD-L1 resistance in cancer through LAIR1-dependent CD8(+) T cell exhaustion, Nat. Commun. 11 (2020) 4520. https://10.1038/s41467-020-18298-8.
[54] J. Xie, X. Gui, M. Deng, H. Chen, Y. Chen, X. Liu, Z. Ku, L. Tan, R. Huang, Y. He, B. Zhang, C. Lewis, K. Chen, L. Xu, J. Xu, T. Huang, X.C. Liao, N. Zhang, Z. An, C. C. Zhang, Blocking LAIR1 signaling in immune cells inhibits tumor development, Front. Immunol. 13 (2022) 996026. https://10.3389/fimmu.2022.996026.
[55] A. Kennedy, E. Waters, B. Rowshanravan, C. Hinze, C. Williams, D. Janman, T.A. Fox, C. Booth, A.M. Pesenacker, N. Halliday, B. Soskic, S. Kaur, O.S. Qureshi, E. C. Morris, S. Ikemizu, C. Paluch, J. Huo, S.J. Davis, E. Boucrot, L. Walker, D.M. Sansom, Differences in CD80 and CD86 transendocytosis reveal CD86 as a key target for CTLA-4 immune regulation, Nat. Immunol. 23 (2022) 1365–1378. https://10.1038/s41590-022-01289-w.
[56] A. Julia, I. Bonafonte-Pardas, A. Gomez, M. Lopez-Lasanta, M. Lopez-Corbeto, S.H. Martinez-Mateu, J. Llados, I. Rodriguez-Nunez, R.M. Myers, S. Marsal, Targeting of the CD80/86 proinflammatory axis as a therapeutic strategy to prevent severe COVID-19, Sci. Rep. 11 (2021) 11462. https://10.1038/s41598-021-90797-0.